

Supplemental Data

Supplemental Figure 1. Mtb slows its growth in response to acidic pH. A. Mtb grown in the rich medium 7H9 slows growth at acidic pH, but does not arrest its growth. **B.** Mtb grown in minimal medium containing 10 mM glycerol arrests its growth at pH 5.7. The threshold for slowed growth is pH 6.4, the same pH at which the *phoP* pathway is induced by acidic pH. **C.** Mtb grown on minimal medium containing 10 mM glycerol or 10 mM glucose, or both carbon sources combined, exhibit arrested growth at pH 5.7. Error bars represent the standard deviation and the data are representative of three independent experiments.

Supplemental Figure 2. Nine day growth curves that correspond to the endpoint point data summarized in Figure 1A.

Supplemental Figure 3. Long-term growth curves examining Mtb growth and medium pH. A. Growth of Mtb was examined over 36 days in 10 mM glycerol or 10 mM pyruvate at acidic and neutral pH. At stationary phase, Mtb accumulates a greater total biomass in glycerol at pH 7.0 as compared to pH 5.7, whereas, a similar total biomass is observed in pyruvate at both pH 7.0 and 5.7. **B.** pH of the culture supernatants was measured at the end of the time course. The media initially buffered at pH 7.0 with 100 mM MOPS or pH 5.7 with 100 mM MES maintained their pH through the course of the experiment.

Supplemental Figure 4. Carbon source specific growth arrest at acidic pH is species specific. A. *Mycobacterium smegmatis* does not arrest its growth at

acidic pH on any of the tested carbon sources. Growth was initiated at a starting density of 0.05 OD₆₀₀ (horizontal dotted line) and growth was measured at Day 6. **B.** Growth arrest phenotypes at day 9 are generally conserved amongst diverse strains of Mtb. H37Rv, Erdman, HN878, and CDC1551 all exhibit carbon source specific growth arrest on glycerol and pyruvate enables growth. Error bars represent the standard deviation and the data are representative of three individual experiments. * shows that in pyruvate at acidic pH, H37Rv, Erdman and HN878 have significantly lower growth ($p < 0.01$ using a student's t-test) as compared to CDC1551.

*Supplemental Figure 5. NAD(P)/NADPH ratios at acidic and neutral pH in 10 mM glycerol or 10 mM pyruvate. A. NAD⁺ concentration. B. NADH concentration C. NAD⁺/NADH ratio, D. NADP⁺ concentration. E. NADPH concentration F. NADP⁺/NADPH ratio. Error bars represent the standard deviation of three biological replicates and two technical replicates. Error bars represent the standard deviation of three biological replicates each calculated from the average of two technical replicates. The data are representative of three individual experiments. * $p < 0.05$ using a student's t-test.*

Supplemental Figure 6. RNA-seq scatter plots demonstrate significant pH- and carbon-source specific transcriptional adaptations. A. Differential expression of genes at pH 7.0 in pyruvate as compared to glycerol (genes induced or repressed in the presence of pyruvate). B. Differential expression of genes in glycerol at pH 5.7 as compared to pH 7.0. (genes are induced or repressed at pH

5.7). **C.** Differential expression of genes in pyruvate at pH 5.7 as compared to pH 7.0. (genes are induced or repressed at pH 5.7). **D.** Differential expression of genes at pH 5.7 in pyruvate as compared to glycerol (genes induced or repressed in the presence of pyruvate). Scatter plots represent the average of 2 biological replicates. The red spots have a p-value <0.05. The triangles are beyond the scale of the axis.

Supplemental Figure 7. Genes that are induced or repressed by acidic pH in a carbon source independent and dependent manner. **A.** Venn diagram of genes that induced at acidic pH by glycerol or pyruvate. **B.** Venn diagram of genes that are repressed at acidic pH by glycerol or pyruvate. These Venn diagrams correspond to the gene lists presented in Supplemental Table 5. **C.** RNA-seq expression data for *pks2*, *icl1*, and *pckA* was confirmed using quantitative real-time PCR and previously described methods(Abramovitch *et al.*, 2011). The acidic pH induction of *pks2* was confirmed to be carbon source independent, and acidic pH induction of *icl1* and *pckA* was confirmed to be enhanced in pyruvate.

Supplemental Figure 8. Summary model of growth and transcriptional profiling experiments examining pH-driven remodeling of physiology. Carbon sources in red or blue are permissive or non-permissive for growth at acidic pH, respectively. Genes in red or blue are induced or repressed at pH 5.7, respectively. Genes that are underlined are significantly more differentially regulated in pyruvate as compared to glycerol. Metabolic pathways shaded in red

are favored at acidic pH. This figure was modeled after that by Muñoz-Elías and McKinney (Munoz-Elias & McKinney, 2006).

Supplemental Figure 9. Acidic pH modulates Mtb lipid metabolism and carbon metabolism. A. 2D TLC to examine ^{14}C acylated trehaloses in WT Mtb at pH 7.0 and pH 5.7. The first dimension is chloroform:methanol:water (100:14:0.8 v/v/v) and in the second dimension chloroform:acetone:methanol:water (50:60:2.5:3, v/v/v/v). Bands 1, 2, 3 and 4 are predicted to be sulfolipid, trehalose dimycolate (TDM), di- or polyacyltrehaloses (DAT or PAT) or trehalose monomycolate (TMM), respectively, based on published studies (Bhatt *et al.*, 2007). **B.** Analysis of PDIM accumulation at acidic pH. The TLC was developed in petroleum ether:acetone (98:2, v/v), and PDIM was identified based on the relative position on the TLC and previous mass spectrometry-based characterization (Abramovitch *et al.*, 2011). **C.** Relative ratios of lipids in Figure 6A and B relative to WT at pH 7.0. Quantification was performed using the ImageJ software.

Supplemental Figure 10. Nine day time course examining growth of Mtb in response to 3NP. A. Wild Type. **B.** ΔphopPR . **C** ΔphopPR complemented. The end-point data are presented in Figure 6C.

Supplemental Table 1: Gene expression tables of Mtb grown at pH 7.0 in pyruvate as compared to glycerol.

Supplemental Table 2: Gene expression tables of Mtb grown in glycerol at pH 5.7 as compared to pH 7.0.

Supplemental Table 3: Gene expression tables of Mtb grown in pyruvate at pH 5.7 as compared to pH 7.0.

Supplemental Table 4: Gene expression tables of Mtb grown at pH 5.7 in pyruvate as compared to glycerol.

Supplemental Table 5: Gene expression tables of genes highlighted in Figures 5 and S7.

Supplemental Methods:

NAD⁺/NADH and NADP⁺/NADPH cycling assays

Quantification of NAD⁺/NADH was performed using an assay adapted from San and colleagues (San *et al.*, 2002). Mtb cultures were grown at 37 °C in T-75 vented, standing tissue culture flasks in 40 ml of MMAT medium seeded an initial OD of 0.1. Four conditions were examined: 1) 10 mM Glycerol, pH 7.0, 2) 10 mM Glycerol pH 5.7, 3) 10 mM Pyruvate pH 7.0 and 4) 10 mM Pyruvate pH 5.7. Following 3 days incubation, the equivalent of 20 mL of culture normalized at OD 0.1 was pelleted for each culture by centrifugation at 3300 rpm for 10 minutes. Samples were washed in 1 ml of 10% glycerol and pelleted at 15,000 rpm for 5 minutes. The supernatant was removed and pellets flash frozen twice in a dry ice ethanol bath. The pellet was resuspended in 100 µl 0.1 HCl for NAD⁺ extraction or 100 µl 0.025 M NaOH + 1 mM EDTA for NADH extraction and heated at 50°C for 20 minutes. Samples were neutralized using 0.3 M KHPO₄. 95 µl of cycling reaction mixture (equal parts ethanol, 4.2 mM MTT, 40 mM EDTA, and 1 M bicine pH 8.0, and twice the volume of 16.6 mM phenazine ethosulfate (PES)) was combined with 100 µl of sample extract and 5 µl of yeast alcohol dehydrogenase (300 units/mL). Absorbance at 570 nm was measured every minute for 10 minutes at 30°C. Standard curves were prepared for both NAD⁺ and NADH under the same acid and base extraction procedure, respectively. Quantification of NADP⁺/NADPH was performed using the above method, with the enzyme and substrate being substituted with glucose-6-phosphate dehydrogenase and glucose-6-phosphate, respectively.

References:

Abramovitch, R.B., K.H. Rohde, F.F. Hsu & D.G. Russell, (2011) *aprABC*: a *Mycobacterium tuberculosis* complex-specific locus that modulates pH-driven adaptation to the macrophage phagosome. *Mol Microbiol* **80**: 678-694.

Bhatt, K., S.S. Gurcha, A. Bhatt, G.S. Besra & W.R. Jacobs, (2007) Two polyketide-synthase-associated acyltransferases are required for sulfolipid biosynthesis in *Mycobacterium tuberculosis*. *Microbiology* **153**: 513-520.

Munoz-Elias, E.J. & J.D. McKinney, (2006) Carbon metabolism of intracellular bacteria. *Cell Microbiol* **8**: 10-22.

San, K.Y., G.N. Bennett, S.J. Berrios-Rivera, R.V. Vadali, Y.T. Yang, E. Horton, F.B. Rudolph, B. Sariyar & K. Blackwood, (2002) Metabolic engineering through cofactor manipulation and its effects on metabolic flux redistribution in *Escherichia coli*. *Metabolic engineering* **4**: 182-192.

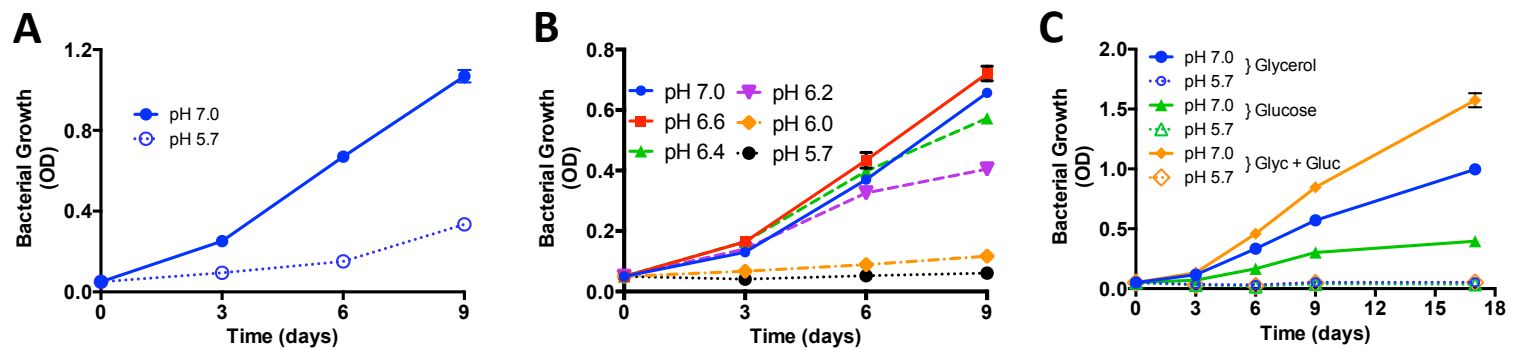


Figure S1

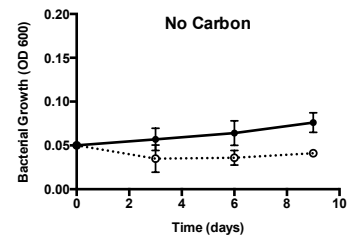
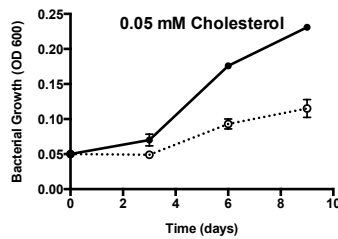
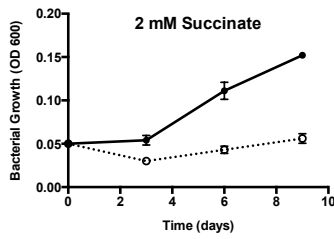
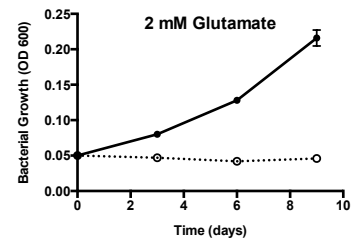
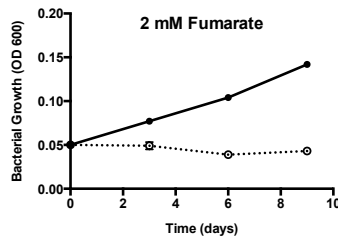
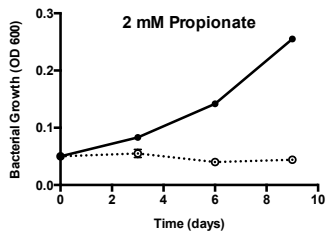
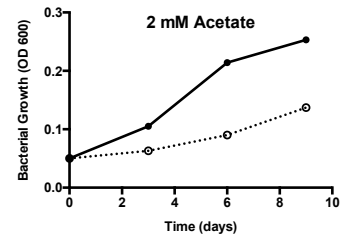
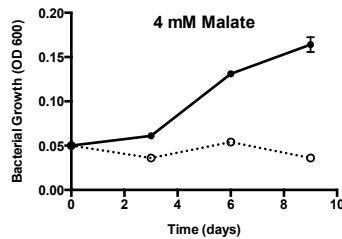
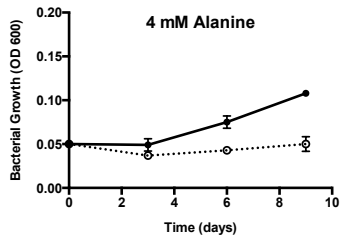
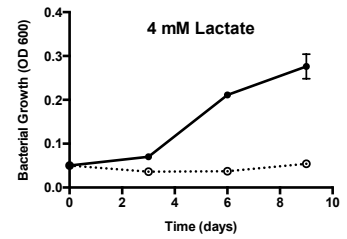
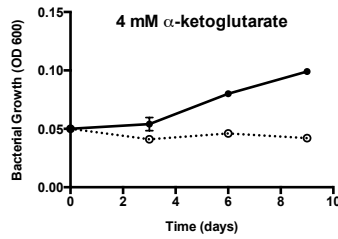
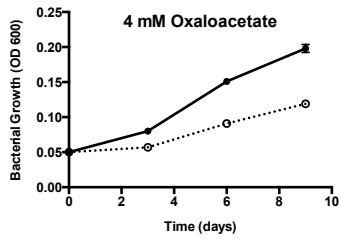
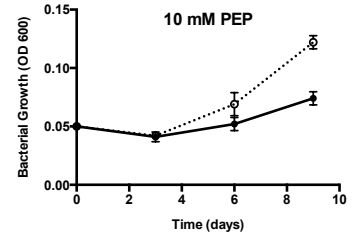
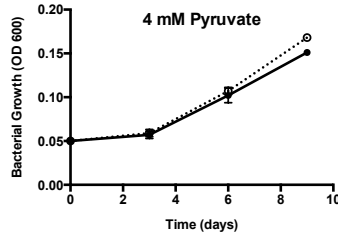
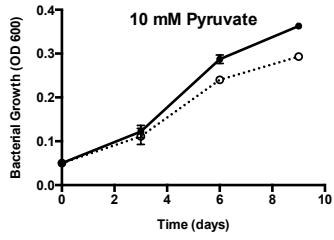
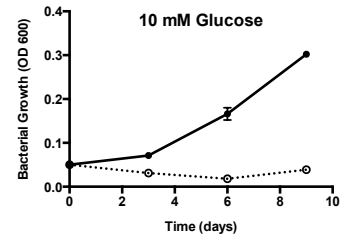
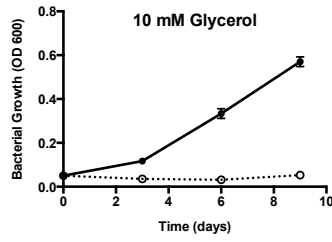
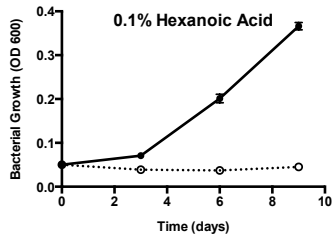


Figure S2

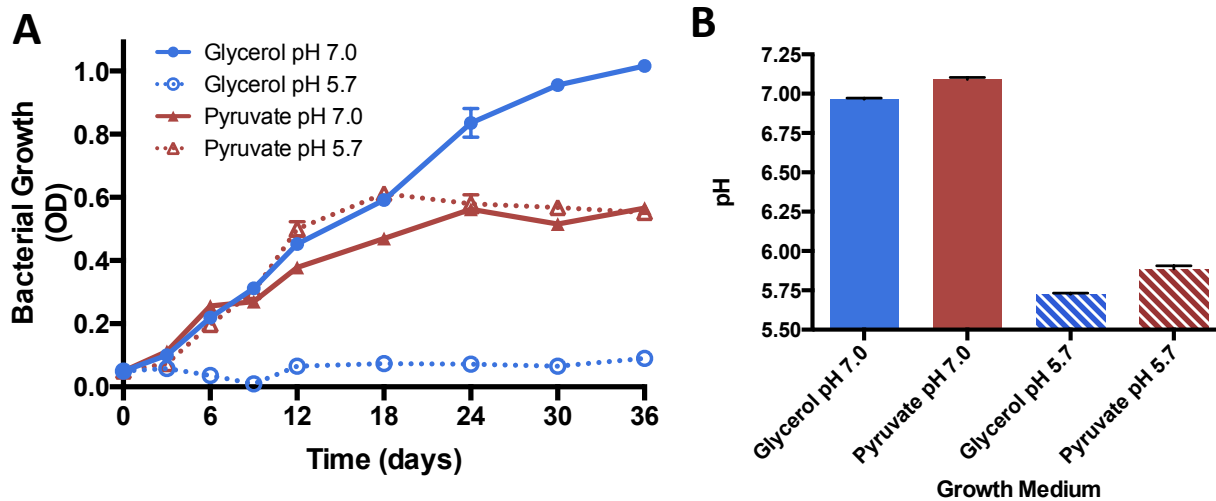


Figure S3

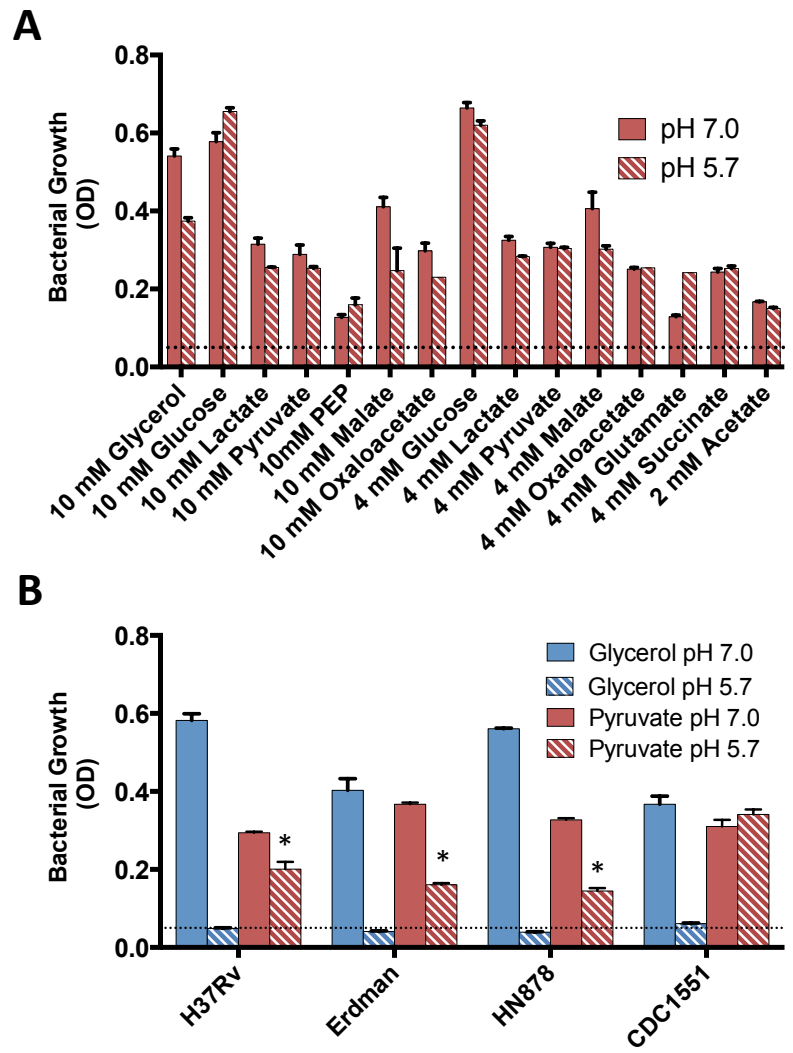


Figure S4

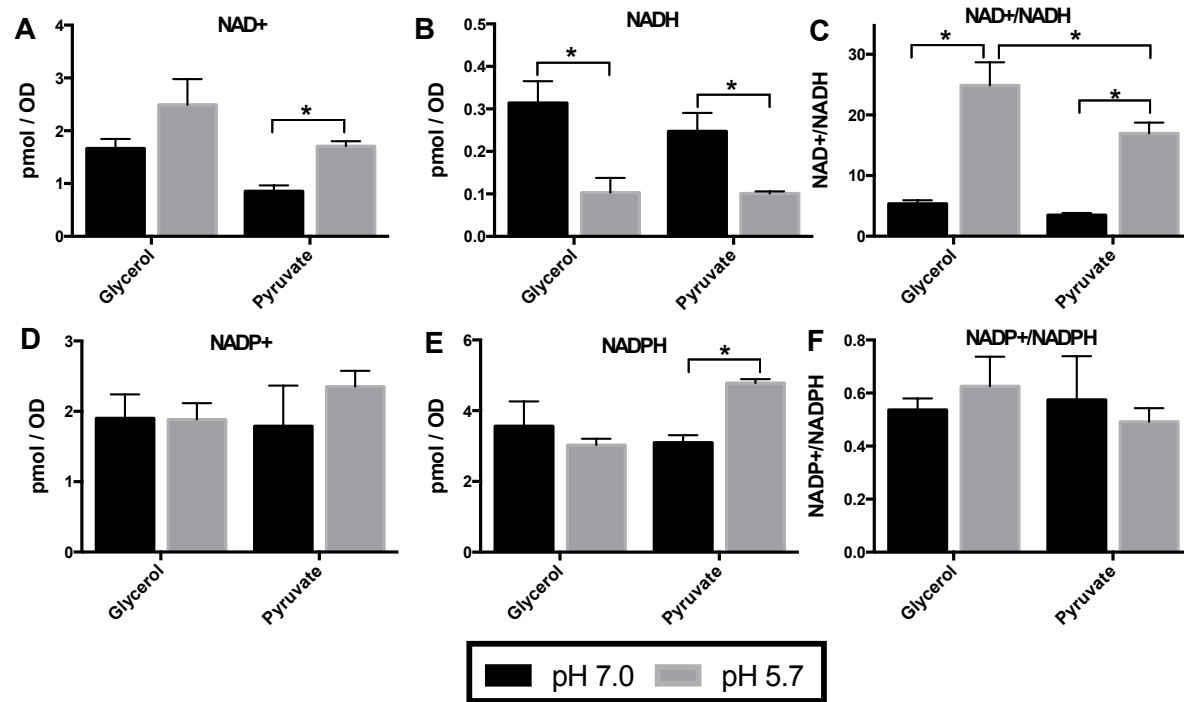


Figure S5

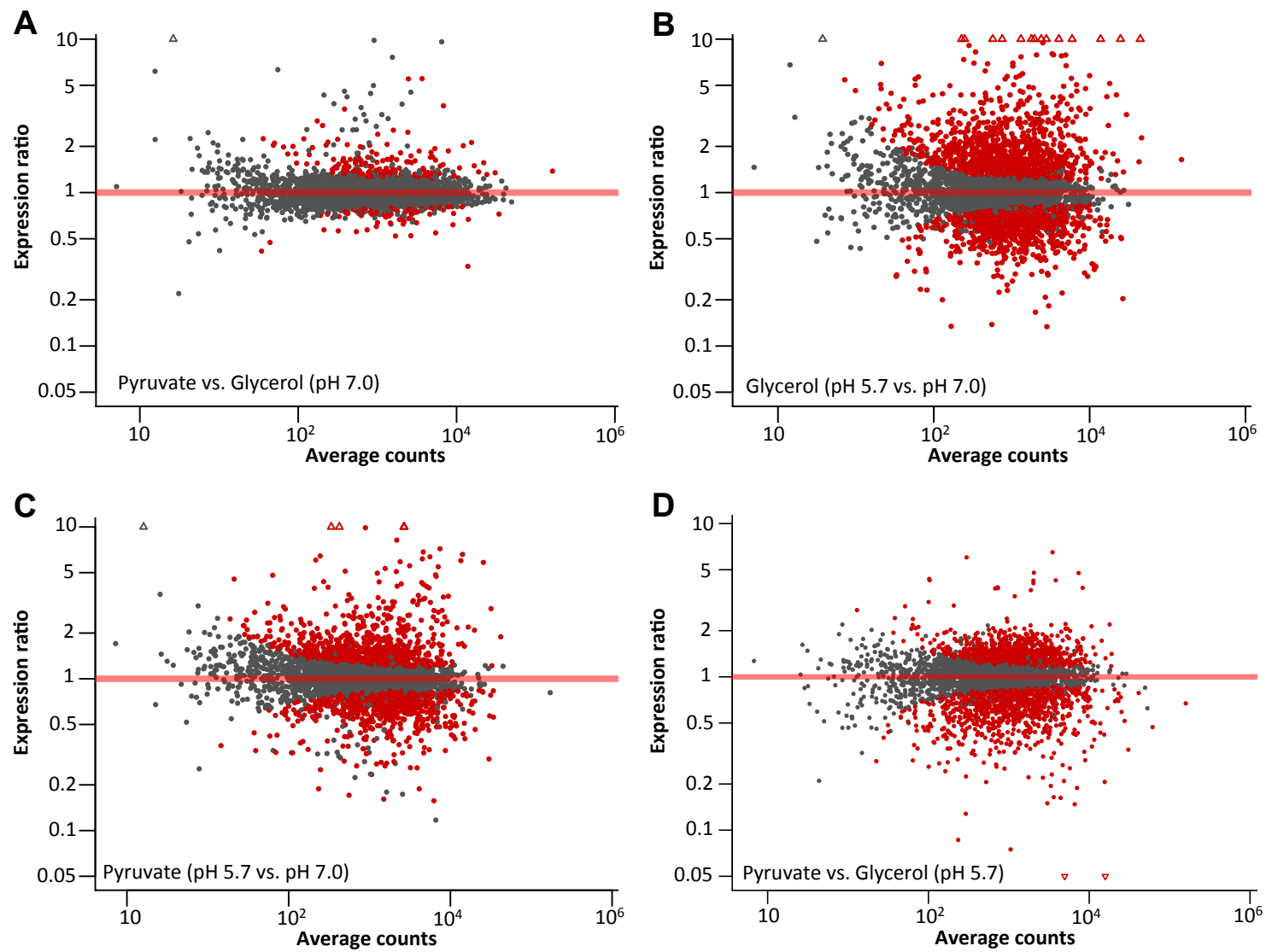


Figure S6

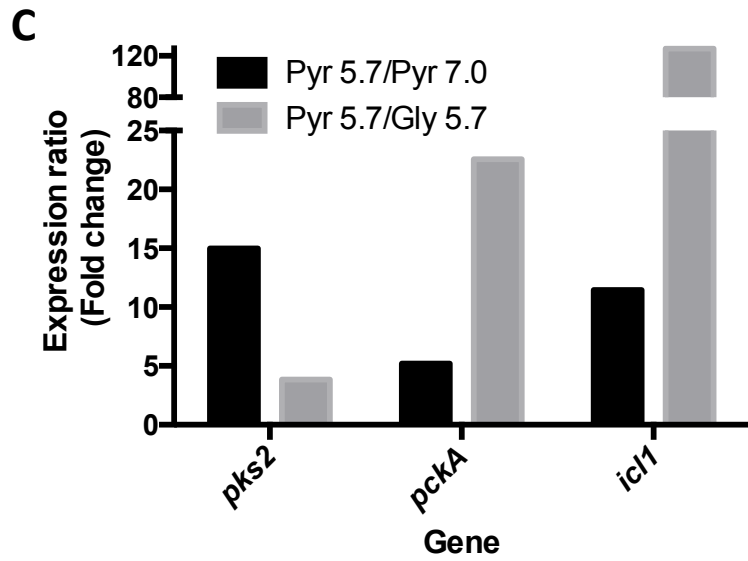
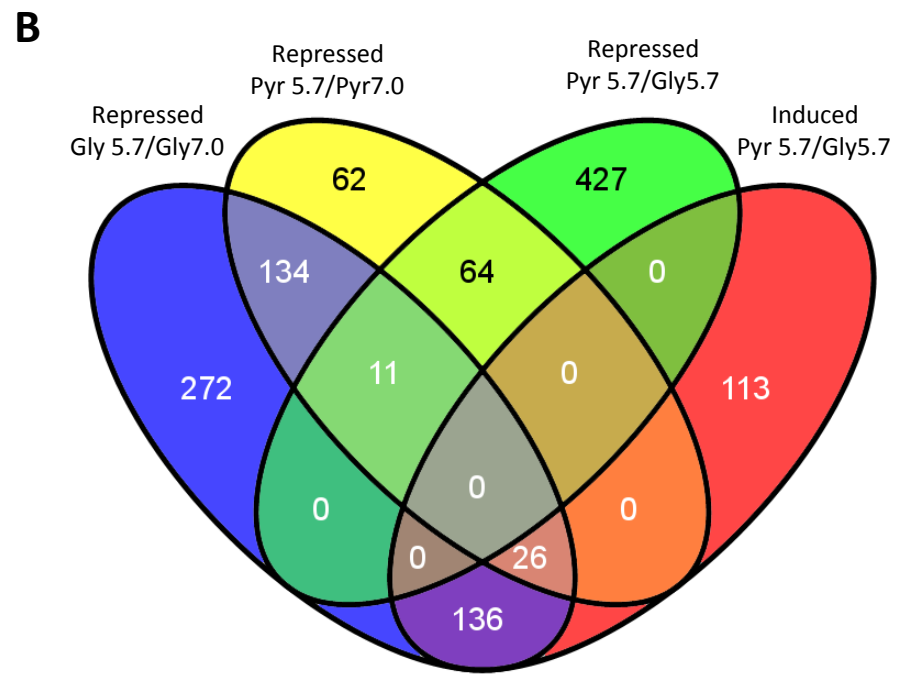
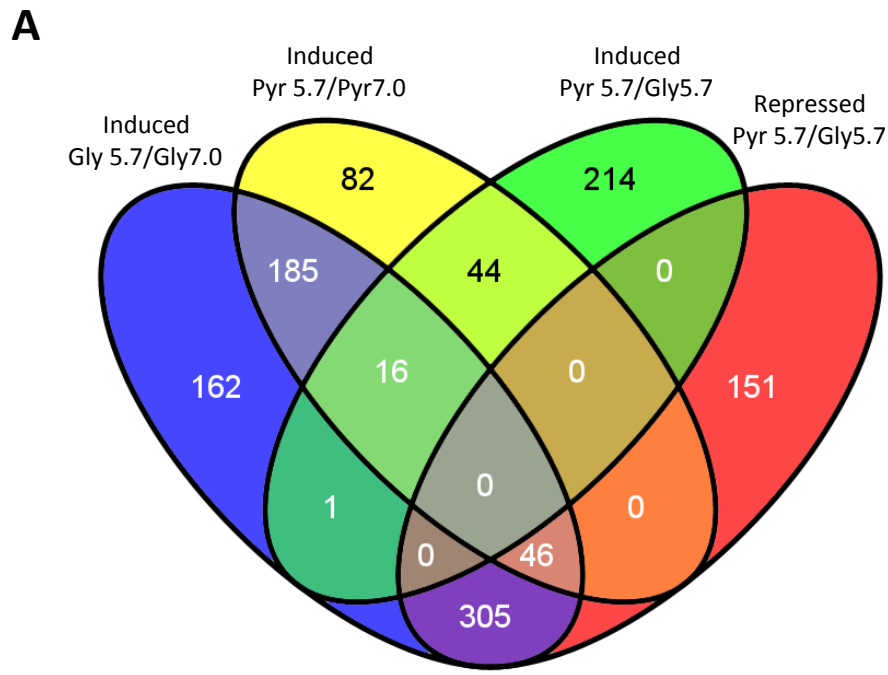


Figure S7

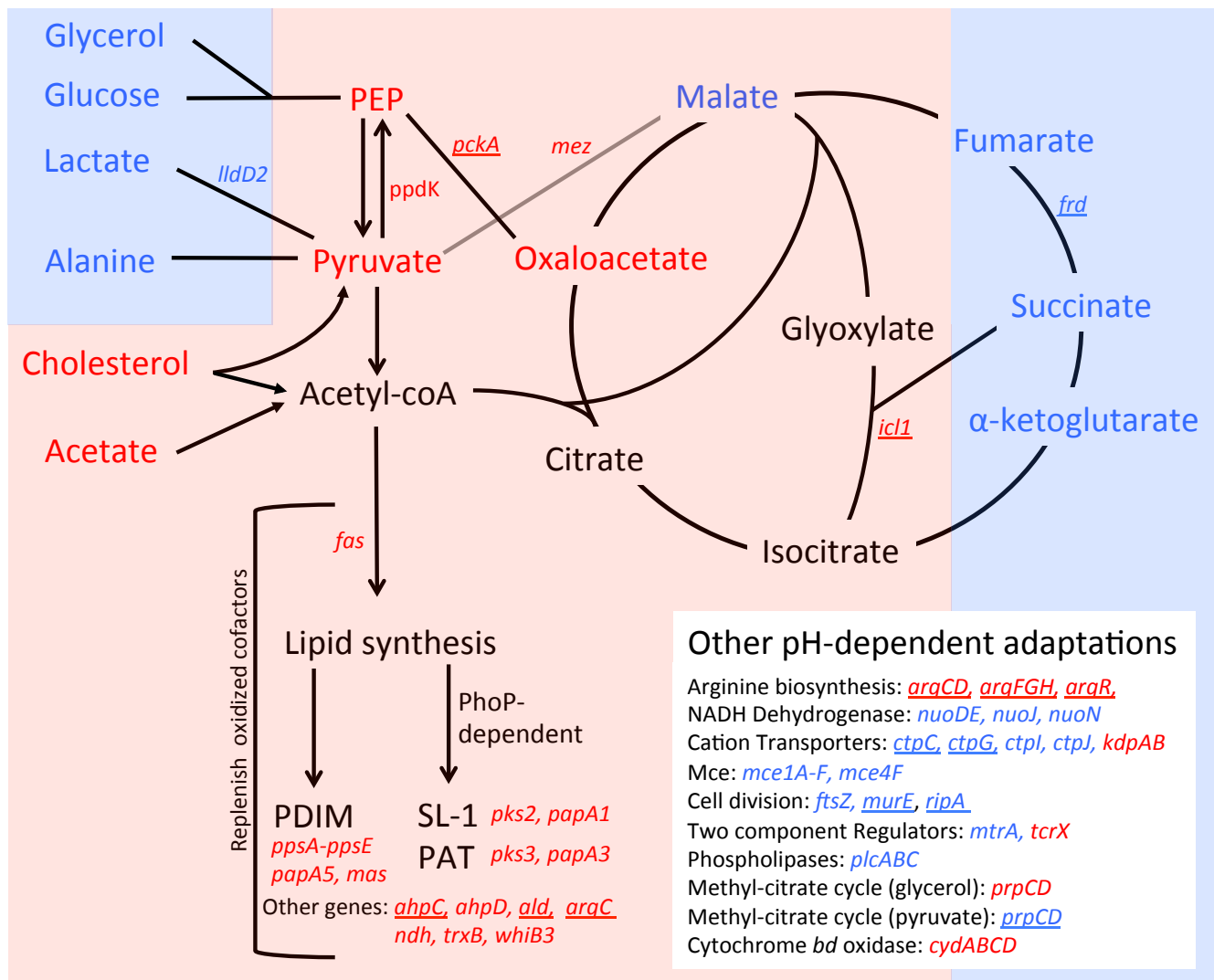


Figure S8

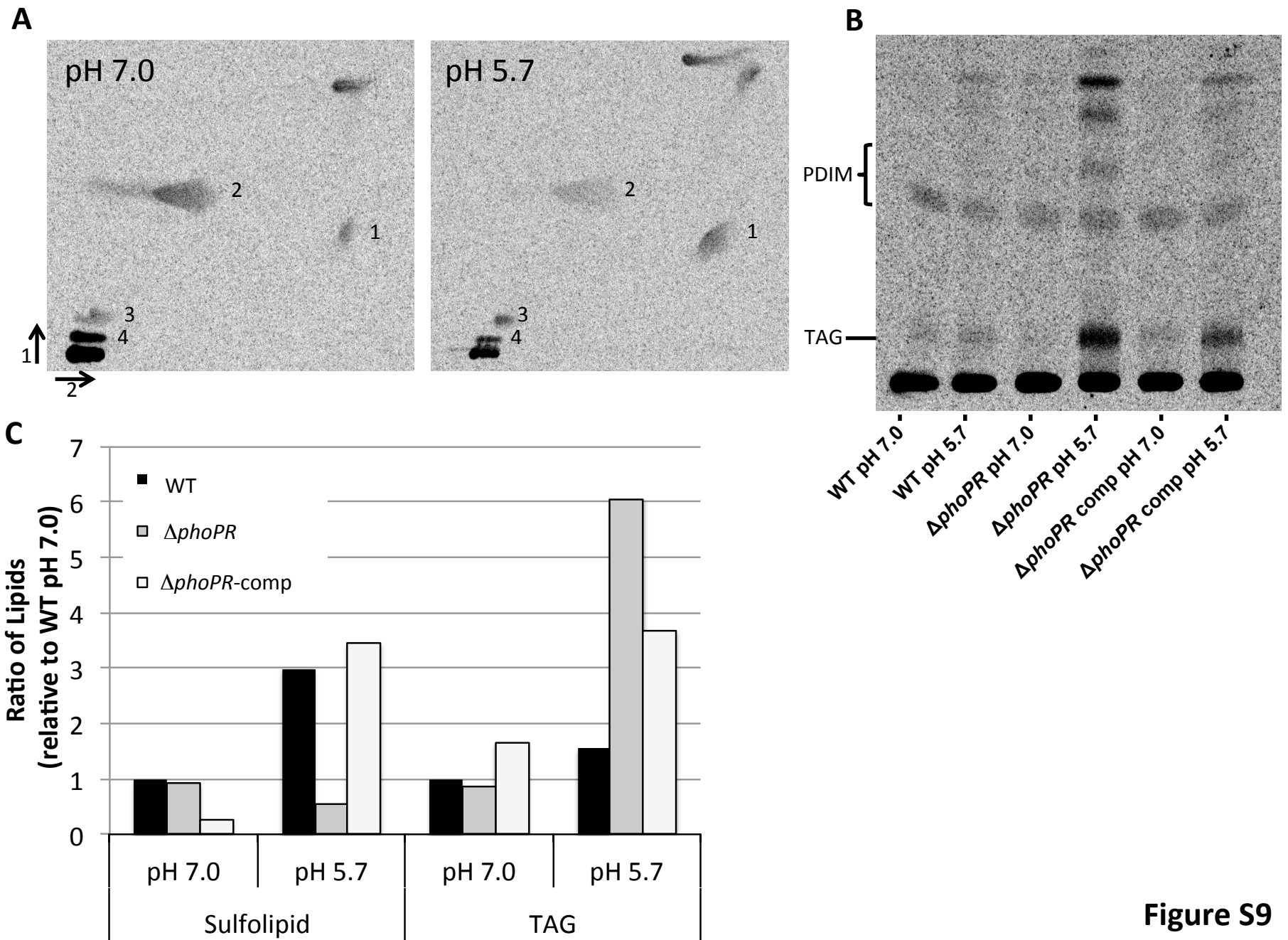


Figure S9

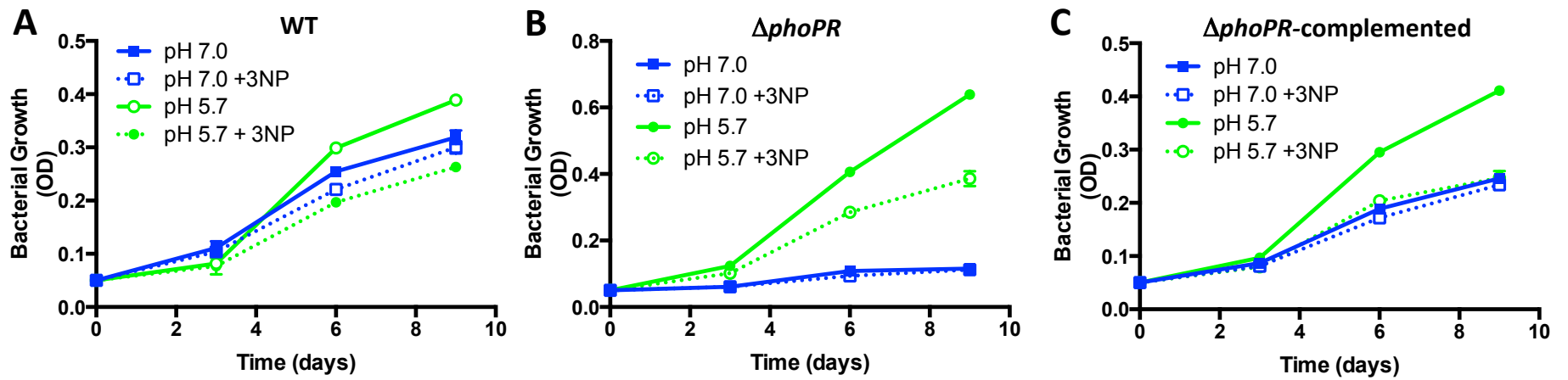


Figure S10